ACTA
PALAEONTOLOGICA
POLONICA

Instytut Paleobiologii PAN
ul. Twarda 51/55
PL-00-818 Warszawa, Poland

e-mail: app@twarda.pan.pl; tel.: (+48 22) 697 88 79; fax: (+48 22) 620 62 25

New specimens of the crested theropod dinosaur *Elmisaurus rarus* from Mongolia

PHILIP J. CURRIE, GREGORY F. FUNSTON, and HALSZKA OSMÓLSKA†

Currie, P.J., Funston, G.F., and Osmólska, H. 201X. New specimens of the crested theropod dinosaur *Elmisaurus rarus* from Mongolia. *Acta Palaeontologica Polonica* XX (X): xxx-xxx. http://dx.doi.org/10.4202/app.00130.2014

New specimens of *Elmisaurus rarus* from the Upper Cretaceous of Mongolia (Nemegt Formation) preserve bones not previously found in "elmisaurids" that help elucidate their relationships to *Leptorhynchos elegans* and other oviraptorosaurs. *Elmisaurus rarus* and the North American *Leptorhynchos elegans* are known from numerous but incomplete specimens that are closely related to, but nevertheless clearly distinguished from, *Chirostenotes pergracilis* and *Epichirostenotes curriei*. These specimens include the first known cranial bone attributed to *Elmisaurus*, the frontal, which clearly shows this animal had a cranial crest (most of which would have been formed by the nasal bones). The first vertebrae, scapula, femora, and tibiae from *Elmisaurus* are also described. The Elmisaurinae can be distinguished from the Caenagnathinae by the coossification of the tarsometatarsus and smaller size at maturity. Examination of oviraptorosaur hindlimbs reveals four distinct morphotypes, possibly attributable to paleoecological differences.

Key words: Dinosauria, Theropoda, Upper Cretaceous, oviraptorosauria, Caenagnathidae, Elmisaurinae, Mongolia**.**

Philip J. Currie [philip.currie@ualberta.ca] and Gregory F. Funston [funston@ualberta.ca], Biological Sciences CW405, University of Alberta, Edmonton, Alberta T6G 2E9, Canada.
Halszka Osmólska, Instytut Paleobiologii, Polska Akademia Nauk, ul. Twarda 51/55, 00-818 Warszawa, Poland. Passed away on the 31st of March 2008.

Received 6 October 2014, accepted 3 January 2015, available online 27 January 2015.

Introduction

Discovered originally by the Polish-Mongolian Palaeontological Expedition of 1970, the remains of *Elmisaurus rarus* Osmólska, 1981 consisted mostly of hand and foot elements derived from three specimens (Osmólska 1981). Some additional skeletal elements, mostly fragmentary, were not included in the original description because they were not considered diagnostic when the original paper was written.

Osmólska (1981) noted that the manual elements of *Elmisaurus* show strong similarities with *Chirostenotes pergracilis* Gilmore, 1924, and the foot elements with *Macrophalangia canadensis* Sternberg, 1932. This suggested to her that *Chirostenotes* and *Macrophalangia* were congeneric, a suspicion confirmed later by the discovery of a specimen in Dinosaur Provincial Park (Currie and Russell 1988).

Elmisaurus remains were subsequently recognized in North America (Currie 1989), although they were attributed to a different species ("*Elmisaurus*" *elegans*). These species, along with *Chirostenotes pergracilis*, were assigned (Currie 1990, 1997) to the family Elmisauridae, which Osmólska (1981) had established. The discovery in Asia of small mandibles comparable with North American caenagnathids prompted Currie et al. (1993) to speculate that they were from an animal like *Elmisaurus*. This implied that Elmisauridae and Caenagnathidae might be synonymous. The inclusion of *Chirostenotes* in the Elmisauridae was shown to be incorrect when it was established that this genus was congeneric with the caenagnathid oviraptorosaur *Caenagnathus* (Sues 1997), which has left open the question of whether or not the family Elmisauridae is synonymous with Caenagnathidae.

In 2000, an expedition to Mongolia recovered additional *Elmisaurus rarus* specimens from Western Sayr (Gradziński et al. 1977: fig. 4) of the Nemegt locality. The four specimens (MPC-D 102/006–009) were found in the same region, but were separated from each other by at least 100 m. These specimens include previously unknown remains of cranial and postcranial elements that are described in this paper. Additional specimens were found in 2001 and 2002 in Central and Western Sayrs.

Additional postcranial bones of the *Elmisaurus rarus* specimen ZPAL MgD-I/98, some of which were prepared after the initial description (Osmólska 1981) of the specimen, are also described. This specimen and others described by Osmólska (1981) were collected in Northern Sayr of the Nemegt Locality, although precise information on where they were collected is unknown. Elmisaurid specimens have not been recovered from Eastern Sayr of the Nemegt locality, nor from the other major Nemegt Formation sites (including Altan Uul, Bugiin Tsav, Hermiin Tsav).

Additional specimens from Alberta (Funston et al. in press) show that *Elmisaurus rarus* and *Leptorhynchos elegans* Longrich, Barnes, Clark, and Millar, 2013 are closely related and belong to their own subfamily within Caenagnathidae.

Institutional abbreviations.—AMNH, American Museum of Natural History, New York, USA; CMN, Canadian Museum of Nature, Ottawa, Canada; MOR, Museum of the Rockies, Bozeman, Montana, USA; MPC-D, Mongolian Paleontological Center (dinosaur collection), Mongolian Academy of Sciences, Ulaan Baatar, Mongolia; RSM, Royal Saskatchewan Museum, Regina, Saskatchewan, Canada; TMP, Royal Tyrrell Museum of Palaeontology, Drumheller, Alberta, Canada; UALVP, University of Alberta

Laboratory of Vertebrate Paleontology, Edmonton, Alberta, Canada; YPM, Yale Peabody Museum, New Haven, USA; ZPAL MgD-I, Institute of Paleobiology, Polish Academy of Sciences, Warsaw, Poland.

Materials and methods

All specimens were collected under permits from the Government of Mongolia using standard palaeontological field techniques, and are curated in the collections of the Mongolian Paleontological Center in Ulaan Baatar and the Institute of Paleobiology in Warsaw. Measurements of specimens were taken with digital calipers. Mongolian place name spellings follow those suggest by Benton (2000).

Systematic palaeontology

Dinosauria Owen 1842

Saurischia Seeley 1888

Theropoda Marsh 1881

Oviraptorosauria Barsbold 1976

Caenagnathoidea R.M. Sternberg 1940

Caenagnathidae Sternberg 1940

Elmisaurinae Osmólska 1981

Genus *Elmisaurus* Osmólska, 1981

Type species: *Elmisaurus rarus* Osmólska, 1981; Nemegt Formation, Nemegt locality, Mongolia.

Elmisaurus rarus Osmólska, 1981

Fig. 1–11.

Material.—MPC-D 102/006: right tarsometatarsus. Nemegt Formation (Cretaceous), Mongolia, Western Sayr of Nemegt locality (43°30’451” N, 101°2’441” E), found by Demchig Badamgarav (September 8, 2000), collected by D. Badamgarav and PJC (field number PJC2000.01). MPC-D 102/007: partial skeleton including skull fragment, one cervical and one dorsal vertebra (incomplete), fragments of at least two more vertebrae, three rib heads (all left), rib shaft fragments, gastralia fragments, left manual phalanges II-2 (distal part), II-3, III-1 and III-3, proximal end of right femur, both tibiae, and parts of the left metatarsals II and IV, a partial right metatarsal III, and pedal phalanges I-1 and I-2. Nemegt Formation (Cretaceous), Mongolia, Western Sayr of Nemegt locality (43°30’430”N, 101°2’420”E), found by Paul Sealey (September 8, 2000), collected by Demchig Badamgarav, PJC, and others (field number PJC2000.02). MPC-D 102/008: isolated left metatarsal IV. Nemegt Formation (Cretaceous), Mongolia, Western Sayr of Nemegt locality (43°30’160”N, 101°3’040”E), found by Demchig Badamgarav, (September 9, 2000), collected by Eva Koppelhus (September 10, 2000; field number PJC2000.03). MPC-D 102/009: proximal end of right tarsometatarsus. Nemegt Formation (Cretaceous), Mongolia, Western Sayr of Nemegt locality (43°30’30”N, 101°2’71”E), found and collected by PJC (September 15, 2001; field number PJC2001.08). MPC-D 102/010: tibia, vertebra. Nemegt Formation (Cretaceous), Mongolia, Central Sayr of Nemegt locality (43°30’16”N, 101°3’04”E), found and collected by J. Ed. Horton (August 2, 2002; field number PJC2002.40). ZPAL MgD-I/98: elements of the right

manus and right pes (described by Osmólska 1981), ventral halves of centra of two mid-sacral vertebrae, proximal part of right scapula, proximal parts of right and left pubes, proximal part of right ischium and incomplete shafts of right and left ischia (obturator processes broken off), damaged shaft of right femur, proximal portion of left femur, incomplete right tibia, almost complete left pedal digits (phalanx IV-1 lacks the medial part of the shaft), fragments of ribs and gastralia, and numerous fragments of indeterminate postcranial bones. Nemegt Formation (Cretaceous), Mongolia, Northern Sayr of Nemegt locality.

Description.—An isolated frontal (50.5 mm long) of *Elmisaurus rarus* was found with MPC-D 102/007 (Fig. 1). The identification is based on the presence of ventral depressions for the orbit and brain cavity, and sutures for the laterosphenoid, parietal and postorbital. The bone is less than 2 mm thick and does not appear to be pneumatized. The interfrontal suture is dorsoventrally thin posteriorly (4 mm), dorsoventrally deep (15.2 mm) anteriorly, and lightly striated longitudinally. The nasal contact is a large, deep slot between the interfrontal suture and the orbital margin; the nasal extended posteriorly to a position between the supratemporal openings. There are no obvious sutures for either the prefrontal or the lacrimal, which suggests that the large nasal contact was also at least partially filled by the lacrimal. Unfortunately, the anterolateral tip of the frontal is incomplete. The slot ("nas" on Fig. 1A) is open ventrally almost to the back of the orbit, posterior to which it becomes a depression in the dorsal surface of the frontal. The frontals formed a flat dorsal surface between the upper temporal fenestra. There is a strong suture (7.5 mm long anteroposteriorly; "par" on Fig. 1E) that overlapped the front

of the parietal. In dorsal view, the suture shows that the most anterior margin of the parietal is on the midline. However, a thin process extended anterolaterally along the margin of the frontal to contact the laterosphenoid and postorbital as in most theropods; the suture is only visible in lateral and ventral views. The postorbital process of the frontal is almost perpendicular to the medial orbital margin. This is the widest part of the bone. As in other theropods, the dorsal surface of this process slopes posteroventrally into the supratemporal fenestra. There is a distinct suture posterolaterally with the postorbital bone. The ventral margin of the postorbital process has a transverse groove for the postorbital process of the laterosphenoid. Overall, the postorbital process is similar to those of dromaeosaurids. The domed, ventral surface over the brain has impressions of blood vessels, suggesting the animal was highly encephalized (Osmólska 2004).

Three vertebrae were recovered with MPC-D 102/007 (Fig. 2). An anterior to mid-cervical neural arch is relatively small (21.4 mm long) and tapered, and resembles the third to fifth cervical vertebrae of dromaeosaurids and oviraptorosaurs. The second preserved vertebra is a posterior cervical or anterior dorsal that tapers ventrally into a midline keel. The 26.4 mm long centrum is pierced laterally by a single pleurocoel (sometimes termed a lateral excavation), close to the posterior margin. There is no sign of the suture between the neural arch and centrum, and the coosification suggests that the specimen was mature at the time of death. Only the base of the neural arch is preserved, but on the right side it forms the margin of a large infradiapophysial fossa**.**

The third vertebra of MPC-D 102/007 is an anterior dorsal that lacks the neural spine and transverse processes (Fig. 2). The 27.7 mm long centrum has a large (5 mm) pleurocoel on each side. The anterior edge of the centrum extends ventrally far below the

ventral margin of the vertebra (hypapophysis), and as a consequence the centrum is 22.5 mm high anteriorly. The ventral surface of the hypapophysis is unfinished and suggests that this is a cervicodorsal vertebra, of which there are two or three in oviraptorids and alvarezsaurids. The parapophysis is positioned on the lateral surface at the anteroventral margin of the neural arch, which is consistent with the identification of this vertebra as an anterior dorsal. The neurocentral suture is fused but still discernible for most of its length. An intricate system of laminae and ridges outline the infraprezygapophysial, infradiapophysial, and infrapostzygapophysial pneumatic fossae (Britt 1993). In addition to the highly angled zygapophyses, there are paired hyposphene and hypantrum articulations.

Two fragmentary mid-sacral vertebrae (ZPAL MgD-I/98) show that the ventral surfaces of these vertebrae are almost flat, and that there were no longitudinal furrows along the ventral surfaces of the mid-sacral centra. Such a furrow has been reported in some other maniraptorans (Currie and Russell 1988; Norell and Makovicky 1997), although it is usually present in the more posterior vertebrae. On each of the two sacrals a deep, elongate pleurocoel is present ventrolaterally as in caenagnathids (Currie and Russell 1988), oviraptorids (Balanoff and Norell 2012), tyrannosaurids (Brochu 2002), dromaeosaurs, megaraptorines, ornithomimids, therizinosaurs, and birds (PJC personal observation).

Three of the rib heads, all from the left side, are reasonably well preserved (Fig. 3). The proximal shafts of both the two larger anterior dorsal and the smaller posterior dorsal ribs are hollow and pneumatic. A pneumatopore pierces the base of the lateral surface of the web joining the tuberculum and capitulum in the largest specimen (Fig.

3A). The ribs are generally similar to those of oviraptorosaurs, although the ridges along the anterolateral and posterolateral margins of the proximal part of the shaft are more pronounced.

There is a fragment of scapula preserved in specimen ZPAL MgD-I/98 (Fig. 4). It represents a proximal portion of the bone that has an almost complete glenoid surface and most of the basal portion of the acromial process. The latter is thick across the base and inclines laterally, which suggests that its missing distal part might provide an attachment surface for the clavicular epicleideum. The supraglenoid ridge is not pronounced. Just above the margin of the glenoid and close to the coracoscapular suture, there is a small irregular depression on the lateral surface of the scapula with two to three tiny foramina. On the ventromedial side of the scapular fragment, there is a small nutrient foramen positioned close to the glenoidal surface. The portion of the ventral margin adjoining to the glenoid is rough and thick where it forms an elongate tuberosity.

As only the proximal portion of the bone is preserved (Fig. 4A), the relationship of the scapula to the rib cage, and orientation of the glenoid, whether ventral or lateral, cannot be shown beyond doubt. In theropods with ventrally (or ventroposteriorly) facing glenoids, the scapular portion of the glenoid faces anteroventrally as in *Gallimimus bullatus* Osmólska, Roniewicz and Barsbold 1972, and the oviraptorids *Citipati* sp. nov. Clark, Norell, and Rowe, 2002 (MPC-D 100/42), *Conchoraptor gracilis* Barsbold, 1986 (ZPAL MgD-I/099), and *Ingenia yanshini* Barsbold, 1981 (MPC-D 100/30). In this specimen of *Elmisaurus rarus* (ZPAL MgD-I/98), the glenoid faces somewhat lateroventrally as in dromaeosaurids (Jasinoski et al. 2006), *Epichirostenotes* (Funston and Currie, in press) and some therizinosaurs, which clearly have more lateral

orientations to their glenoids (Perle 1979; Kirkland and Wolfe 2001). The angle to the lateral surface of the blade is approximately 110–120° in *Elmisaurus rarus*, whereas it is around 90° in most other theropods.

In addition to the incomplete manus described by Osmólska (1981), four elements of the hand were recovered with MPC-D 102/007 (Fig. 5). Phalanx II-2 lacks the proximal end, so the total length is unknown. The shaft is 7.3 mm deep and 5.4 mm wide. The distal width is 8.5 mm, which is less than the 10 mm width of ZPAL MgD-I/98 (Osmólska 1981). Like all theropod penultimate phalanges, the collateral ligament pits (foveae ligamentosae) are deep on both sides, and are positioned high on the medial and lateral surfaces of the distal expansion. One ungual phalanx was recovered and lacks only the distal tip. It is about 10% smaller than the ungual described for ZPAL MgD-I/98. The absence of a proximodorsal "lip" is due to breakage (Fig. 5F). The smaller size of MPC-D 102/007 plus the more open curvature, the more distally positioned flexor tubercle and the fact that it articulates well with II-2 indicate that this ungual is phalanx II-3. The ungual described for ZPAL MgD-I/98 (Osmólska 1981) is almost certainly I-2. Phalanges III-1 and III-3 are very slender elements as in other elmisaurids (Osmólska 1981; Currie 1990), and have shaft diameters that are less than two-thirds the width of phalanx II-2. The smaller of the two phalanges has a shallow concave proximal articulation that indicates it is phalanx III-1. The longer phalanx has the high collateral ligament pits that identify it as phalanx III-3. The lateral pit is deeper than the medial one in *Elmisaurus* (Osmólska 1981) and other theropods, indicating that this element is from the left hand. Both third digit phalanges have measurements (Table 1) comparable with, but slightly smaller than, ZPAL MgD-I/98 (Osmólska 1981).

The preserved proximal part of the right pubis of ZPAL MgD-I/98 is associated with the adjoining portion of the ischium forming the ventral margin of the acetabulum. The iliac process of the pubis is broken off, and the ischiadic process is reduced to a thickened lip. Judging by the preserved proximal portion of the left pubic shaft, the shaft may have been somewhat concave anteriorly.

In addition to the proximal part of the right ischium (ZPAL MgD-I/98), there are incomplete shafts of both ischia. They show that the shaft was relatively long and massive, and was only slightly flattened mediolaterally. The distal ends of the shafts are missing, and only the bases of the thin obturator processes are preserved (Fig. 4B).

The head of the left femur (ZPAL MgD-I/98) is cylindrical, somewhat higher than the greater trochanter, and separated from the latter by a broad, shallow depression (Fig. 4). On the posterior surface of the head, there is a wide groove for the capital ligament. The anterior (lesser) trochanter is not complete, but is prolonged into a mediolaterally flattened and anteriorly extended ridge. The preserved thickness of the trochanter is 8 mm. Its shape and orientation suggests that the anterior trochanter was a wing-like rather than a finger-like structure. On the medial side of the shaft, a short distance below the head, there is a shallow, longitudinally oval depression. It corresponds to similarly positioned depressions (or a scars) in ornithurine birds, oviraptorids and ornithomimids (*Gallimimus bullatus*). On the posterolateral surface of the proximal end of the femur, some distance (25–30 mm) below the upper margin of the greater trochanter, there is a large but low protuberance resembling in its position the "posterior trochanter" of *Deinonychus antirrhopus* (Ostrom 1976). Similar protuberances seem be present in

several other theropods, including *Bagaraatan ostromi* (Osmólska 1996) and *Gallimimus bullatus* (Osmólska et al. 1972)

The preserved shaft of the left femur of MPC-D 102/007 has a circumference of 70 mm. A formula (0.8685x + 0.7654, where x and y are the log transformed values of shaft circumference and femoral length respectively; n is 106, and the r^2 value is 0.9808) comparing the femur shaft circumference with femur length in 106 coelurosaurs (Currie 2003), can be used to estimate the length of the femur of MPC-D 102/007 as 233 mm. Using transverse shaft width produces a slightly different result where the estimated value of the femur is 236 mm. Finally, comparison of femoral versus tibial lengths in oviraptorosaurs produces an estimate of 270 mm. The last comparison is tightly constrained (0.9377x + 0.229, where x and y are the log transformed values of femoral and tibial length respectively; n is 43, and the r^2 value is 0.99385). The three measurements were averaged for an estimated femur length of 246 mm. The head of the femur is badly eroded but shows a few characters of interest. Like the head of ZPAL MgD-I/98, the lesser trochanter appears to have been a tall, winglike structure as in most theropods; it does not seem to have been the closely appressed, fingerlike lesser trochanter that is seen in oviraptorids. The shaft circumference suggests that this elmisaurid weighed about 18 kg, using the Anderson et al. (1985) method.

Tibiae (Fig. 6), previously undescribed for *Elmisaurus*, were recovered in two specimens (MPC-D 102/007, MPC-D 102/010). The average length (323 mm) of the right and left tibiae of MPC-D 102/007 suggests that this animal stood approximately 75–80 cm high at the hips. The tibia is somewhat more gracile and elongate than those of similar sized oviraptorids. For example, MPC-D 102/007 (*Elmisaurus*) has a femur

slightly longer (an estimated length of 246 mm) than that (an estimated length of 242 mm) of MPC-D 102/011 (cf. *Ingenia*), but the tibia of MPC-D 102/007 is 25% longer, even though the shaft circumference is 10% less. The unfinished anterior surface of the prominent cnemial crest slopes anteroventrally from the articulation for the medial condyle of the femur (Fig. 6). The cnemial crest is separated from the outer (fibular) condyle by a deep incisura tibialis (Fig. 6D, E). The outer condyle would have contacted more than half the anteroposterior length of the proximal end of the fibula. Its lateral articular surface for the fibula is oriented posterolaterally. This surface is separated from a low ridge extending from the fibular condyle by a shallow concavity. The groove separating the outer and inner condyles is shallow, whereas it tends to be more pronounced in oviraptorids. The rugose edge for the interosseum tibiofibular ligament attachment (Fig. 6G) is more than 4 cm long and oriented anterolaterally. This attachment is 35% of the way down the shaft of the tibia from the proximal end, whereas it is 41% in *Ingenia* (MPC-D 102/011). Just posterior to the distal end of the fibular crest is a small foramen at the distal end of a shallow canal. The canal enters the bone where it forms the lateral corner between the flat anterior and convex posterolateral surfaces of the bone. This is the same in *Ingenia* (MPC-D 100/032, MPC-D 100/033, MPC-D 102/011), *Khaan* (Balanoff and Norell 2012) and other oviraptorosaurs. Distally, the anterior surface of the tibia is flat for its contact with the ascending process of the astragalus. This surface extends medially and laterally into sharply defined ridges, the latter of which is the postfibular flange (Fig. 6F). A groove on the anterior surface of the postfibular flange marks the distal position of the fibula. This groove extends dorsally for almost half the length of the tibia. Its presence shows that the fibula extended to the tarsus and was

closely appressed distally to the lateral edge of the anterior surface of the tibia. A more medial impression shows that the ascending process was at least 65 mm high (20% tibial length). Overall, the anatomy of the tibia is virtually the same as an oviraptorid tibia.

Whereas the tibia of MPC-D 102/007 is only 25% longer than that of an oviraptorid of equivalent size, the tarsometatarsus is relatively longer in *Elmisaurus*; the tarsometatarsus is 70% of femur length in MPC-D 102/007, whereas the average in 22 oviraptorid specimens is only 55% (with a maximum of 60% in the chicken-sized *Yulong mini* [Lu et al. 2013]).

The third and fourth distal tarsals form part of the fused tarsometatarsus in MPC-D 102/006 (Fig. 7A). A third distal tarsal that is not fused to the metatarsus is preserved in association with the second metatarsal of MPC-D 102/007 (Fig. 7B). It caps the posterior third of the proximal articulation of the second metatarsal in both this specimen and that of MPC-D 102/006. The third distal tarsal extends medially to reach the medial margin of the tarsometatarsus, whereas this never happens in oviraptorids. The third distal tarsal also completely covers the proximal articular surface of the third metatarsal. In oviraptorids (for example MPC-D 102/012), the third distal tarsal contacts the lateroposterior margin of the proximal articulation of the second metatarsal, but does not overlap it to any great extent. As the lateral surface of the third distal tarsal is broken (Fig. 7D), it is not possible to know if it was fused to the fourth distal tarsal before death and burial. In MPC-D 102/006, it is fused to both the fourth distal tarsal and posterodistally to both the second and third metatarsals. In outline, it is similar to the same elements in dromaeosaurids, ornithomimids, oviraptorids, and tyrannosaurids. It is 23.5 mm wide, 14.4 mm anteroposteriorly, and covers the posterior half of the proximal

surfaces of the second and third metatarsals. The distal surface of the third tarsal extends posteroventrally around the back of the proximal end of the metatarsals (Fig. 7F). Fusion between the distal tarsals and the metatarsus seems to have proceeded from posterior to anterior (there is no fusion in MPC-D 102/007, posterior fusion in MPC-D 102/006, and complete fusion in ZPAL MgD-I/172). The fourth distal tarsal of MPC-D 102/006 is indistinguishably fused to the third distal tarsal (Fig. 7A), and to metatarsals III, IV, and V. As pointed out by Osmólska (1981), a process projects dorsally from the posterolateral corner of the bone. Unlike any other theropods, the process arches distally to meet the upper end of the fifth metatarsal (Fig. 7G).

The tarsometatarsus in MPC-D 102/006 (Fig. 8A, Table 1), is 15% longer than ZPAL MgD-I/172 but is not as completely fused. Nevertheless in MPC-D 102/006, the third and fourth distal tarsals are fused to each other, and are fused posteriorly to the second to fifth metatarsals. Their anterior margins are still distinct and had not coossified with the second to fourth metatarsals. The second to fourth metatarsals are also coossified posteriorly, but remain distinct in anterior view, which is similar to ZPAL MgD-I/172 (Osmólska 1981). The fifth metatarsal is closely appressed to the fourth but is not fused to it (Fig. 7G). The isolated fourth metatarsal (MPC-D 102/008; Fig. 8C) is 164 mm long (12% longer than ZPAL MgD-I/172) but was not found with either the distal tarsals or the other metatarsals. The posterior part of the proximal surface was damaged when the specimen was found, suggesting that it had been fused posteriorly to the rest of the tarsometatarsus but had broken away before burial and fossilization. The metatarsals of the associated specimen MPC-D 102/007 are about 15% larger than the equivalent parts of ZPAL MgD-I/172, and show no signs of fusion to each other. However, the third distal

tarsal had remained associated with the head of the second metatarsal, suggesting that coossification had begun between these elements. There is therefore some variability in the onset of tarsometatarsal coossification in *Elmisaurus rarus*.

The metatarsus of MPC-D 102/007 (Fig. 8B) is 53% the length of the tibia, which is more elongate than in most oviraptorosaurs (43–48%), but is less than most arctometatarsalian theropods. A section across the mid-length of the metatarsus is deeply concave on the plantar side (Fig. 9). This is because metatarsals II and IV are deep between the extensor and flexor surfaces, especially at tarsometatarsus midheight. As a result, the outer and inner surfaces of these metatarsals are flat, with sharply defined, posteroventral edges. These edges are surmounted by thick and rough ridges along their plantar edges, which are most easily seen in specimens MPC-D 102/006 and ZPAL MgD-I/172. On the fourth metatarsal, a wide but shallow groove is present along approximately the distal fifth of the shaft length. The groove starts somewhat proximal to the lateral fovea ligamentosa and extends upward (proximally) and posteriorly onto the plantar side of metatarsal IV, and distally bounds the thickened portion of the metatarsal edge.

The inner sides of metatarsals II and IV form steep and deep walls (lateral and medial respectively) of a plantar trough (Fig. 9), the narrow bottom of which is formed by the weakly concave surface of metatarsal III. The anterior (dorsal) surface of the metatarsus is concave along about its proximal half, but much less than the plantar surface.

Proximally, there is a short slit between the otherwise tightly connected (or fused) metatarsals III and IV (Osmólska 1981). This slit occurs in ZPAL specimens Mg-D

I/127, 98 (Osmólska 1981: pls. 20: 2; 21: 1) and MPC-D 102/007 (Fig. 8B). Its position is comparable to that of the lateral proximal vascular foramen in modern birds, and *Confuciusornis sanctus* (Chiappe 1999); it probably transmitted a. tarsalis plantaris to the plantar aspect of the foot. On all adequately preserved metatarsi, there is a second, narrower slit located between metatarsal II and the somewhat medially incised metatarsal III (Fig. 8B). This slit is placed more distally than the former, but also cuts through the metatarsus. A similarly located slit is also present in species of *Velociraptor* (HO personal observation). On the anterior (dorsal) surfaces of metatarsals II-IV (Fig. 8A), there is a tripartite protuberance proximally (Osmólska 1981). A similarly placed tubercle is present on metatarsal II in an undetermined dromaeosaurid specimen, probably a species of *Velociraptor* (Norell and Makovicky 1997) and in *Confuciusornis sanctus* (Chiappe et al. 1999). These authors suggest that the tubercle probably marks the insertion of M. tibialis cranialis.

Metatarsals II, III, and IV are the same in the new specimens as they are in ZPAL MgD-I/127 (Osmólska 1981) and little needs to be added to their description. Because the elements of MPC-D 102/007 are separate, some of the contacts between the metatarsals can be seen well. Relatively small (12 mm high, 7 mm anteroposteriorly) facets on metatarsals II and IV contact each other anterior to the proximal end of the third metatarsal (Fig. 8E). The posterior surface of the third metatarsal has two longitudinal ridges (cruciate ridges) that are continuous with the posterior articular ridges. These ridges cross distally, forming a distinctive chiasmata (Fig. 10), as in *Leptorhynchos elegans* from Alberta (Funston et al. in press).

The fifth metatarsal extends proximally beyond the proximal surfaces of the distal tarsals. When found, it formed an ossified arch with the top of the distinctive protuberance (Osmólska 1981) of the fourth distal tarsal. Unfortunately, this fragile arched structure was damaged during collection, although the outline is still visible and it is clear that the fifth metatarsal was fused into the tarsometatarsus as in *Avimimus*. The fifth metatarsal is 70.3 mm long, which is 38% the length of the third. The long tapering fifth metatarsal contacts most of the margin of the ridge along the posterolateral edge of the fourth metatarsal (Fig. 8B) rather than arching away from it as it does in other theropods (Currie and Peng 1993).

Although the first metatarsal was not recovered with MPC-D 102/007, the rest of the digit from the right side was (Fig. 11). The medial collateral ligament pit is deeper than the lateral one in pedal phalanx I-1. In both size and shape, it is similar to I-1 of ZPAL MgD-I/98.

Discussion.—Assignment of *Elmisaurus rarus* to Maniraptora is strongly supported by manus structure (Currie 1990). However, elmisaurines differ from other maniraptorans (except *Chirostenotes pergracilis*) in their slender and elongate first metacarpals, which are short and rather massive in dromaeosaurids, oviraptorids and troodontids (Table 2). Within the third digit, phalanx III-3 is distinctly longer than the more proximal phalanges, and, peculiarly, phalanx III-1 is the most gracile. The manus in *Elmisaurus rarus* and *Chirostenotes pergracilis* are similar in size, and are practically identical in relative proportions (Table 3). The only differences between these taxa concern the more slender first digit and the shapes of the unguals in *Chirostenotes pergracilis* (Zanno and

Sampson 2005: fig. 5a–c), which are more slender, less curved, and have much stronger dorsoproximal lips.

There are also some features in the pes that are exceptional amongst non-avian maniraptorans; the plantar surface of the metatarsus is deeply concave, which results in an arched cross-section in the middle of the metatarsus (Fig. 9). Among other unique features, the tightly attached (or fused) metatarsals III and IV, the large, compound proximal protuberance on the posterior (plantar) surfaces of metatarsals II–IV, and the proximal tuber formed by the fourth distal tarsal and the fifth metatarsal should be mentioned.

A suite of manual and pedal characters ties the elmisaurines to Caenagnathidae, including the elongate metacarpal I, the proximodorsal "lip" on the unguals, and the flat, proximally pinched metatarsal III. Despite these similarities, *Elmisaurus rarus* and *Leptorhynchos elegans* share a number of features that unite them in the Elmisaurinae (Funston et al. in press). The paired cruciate ridges on the posterior surface of metatarsal III (Fig. 10), the fusion of the distal tarsals to each other, and their coossification with metatarsals II, III, and IV, are unique to elmisaurines. Sues (1997) suggested that material assigned to *Elmisaurus* by Currie (1989) was probably synonymous with *Chirostenotes*. The abundance of additional material described here shows that *Elmisaurus* and *Leptorhynchos* ("*Elmisaurus*" of Currie 1989) can be consistently distinguished from *Chirostenotes*. Despite their similar proportions and the distinctive metatarsal III, the fusion of the proximal end of mature elmisaurine tarsometatarsi distinguishes them from *Chirostenotes* (CMN 8538, TMP 1979.020.0001), which have larger but unfused tarsometatarsi. Isolated metatarsals of elmisaurines can be confidently identified based on

the development of the posteromedial ridge of metatarsal II, presence of the cruciate ridges on metatarsal III, the development of the posterolateral ridge of metatarsal IV, and the rugose insertions of *M. tibialis cranialis* on all three. Overall it appears that the elmisaurine foot is a more consolidated unit, with a fused proximal tarsometatarsus at maturity, and a closer association between the shafts of metatarsals II, III, and IV.

The new specimens provide a wealth of new anatomical information. The frontal of *Elmisaurus rarus* suggests it was an encephalized theropod that had a tall nasal crest that extends onto the frontal, possibly analogous to that of *Anzu wyliei* (Lamanna et al. 2014). The vertebrae are similar to those of oviraptorosaurs in general, with large pleurocoels and pneumatized neural arches. The scapulocoracoid is similar to other theropods, but the scapular portion of the glenoid faces lateroventrally, as in some therizinosaurs. The manual unguals are tightly curved, instead of elongate and broadly curved as in other caenagnathids. The tibia is anatomically similar to those of dromaeosaurids and oviraptorosaurs, but is more elongate and gracile. The relatively large protuberance on the posterolateral margin of the proximal surface of the fourth distal tarsal extended to contact the proximal end of the fifth metatarsal, which also protrudes above the articulation between the proximal and distal tarsals. The distal tarsals and metatarsals were probably fused in all mature specimens of *Elmisaurus* and *Leptorhynchos*. The posteromedial and posterolateral longitudinal ridges of metatarsals II and IV are well developed in elmisaurines. This creates a deeply concave posterior margin of the foot in cross section. The third metatarsal has two distinct longitudinal ridges on the posterior surface—one medial and one lateral—that are separated by a

sulcus. In cross section, the shaft of the proximal half of the bone is wider mediolaterally than anteroposteriorly long and is rectilinear rather than triangular.

The lateral orientation of the glenoid of the scapulocoracoid is similar to TMP 1993.051.0001, a caenagnathid from the Dinosaur Park Formation of Alberta. In TMP 1993.051.0001, the biceps tubercle of the coracoid and the deltopectoral crest are expanded (GFF personal observations). The manual structures of *Elmisaurus* and TMP 1993.051.0001 are similar, so perhaps the lateral orientations of the glenoids represent greater forward extensions of the arms to better grasp and manipulate items with the hands. In any case, the lateral position of the glenoid increases the flexibilty of the arm, allowing it to reach farther anteriorly when extended.

Based on foot and leg structure, Oviraptorosauria can be divided up into four major clades (Lamanna et al. 2014). *Caudipteryx* has elongate arctometatarsalian feet showing no fusion of the calcaneum with astragalus, or distal tarsals with metatarsals. *Avimimus*, recovered as the sister taxon to Caenagnathoidea sensu Lamanna et al. (2014), has an astragalocalcaneum fused to the tibia, and the distal tarsals fused to the arctometatarsalian metatarsus (Kurzanov 1981). Caenagnathids have a deep depression on the medial surface of the proximal end of the fibula, fused astragalocalcaneum, elongate arctometatarsalian feet and in the case of elmisaurines at least, the coossified distal tarsals and metatarsals. Oviraptorids lack the depression on the medial surface of the proximal end of the fibula, retain separate astragali and calcanei, and have relatively shorter feet that are not arctometatarsalian. Within each of these groups, proportions of the hindlimb track the changes in morphology. In spite of the elongate, arctometatarsalian nature of the foot in caenagnathids, the tibia is double the length of the metatarsus,

suggesting a cursorial lifestyle. In both *Avimimus* and caenagnathids, elongation of the hindlimb is accompanied by some degree of fusion. In contrast, oviraptorids have short tibiae compared to the femora and a short metatarsi compared to the tibiae, with no fusion of hindlimb elements. This, combined with the non-arctometatarsalian metatarsus, argues against extensive cursoriality in oviraptorids.

It is possible that the morphology of the hindlimb reflects the dietary adaptations of each of these clades. There are some indications of herbivory in members of the Oviraptorosauria, such as the gastroliths in *Caudipteryx* (Ji et al. 1998) and stable isotopes in oviraptorid eggshell (Montanari et al. 2013). Caenagnathids are likely omnivorous (Funston and Currie 2014), and may have retained long legs and elongate hands for prey capture. In contrast, oviraptorids, which may have engaged in crushing (Barsbold 1977, 1983) or strict herbivory (Smith 1992; Montanari et al. 2013), have reduced distal limbs. Longrich et al. (2013) assigned three partial mandibles to *Leptorhynchos*, based on size. These mandibles are similar to those of *Chirostenotes pergracilis* (sensu Longrich et al. 2013; Funston and Currie 2014) and would be equally capable of an omnivorous diet. Although there are numerous problems with these assignments (Funston et al. in press), if the assignment of mandibular material to *Leptorhynchos elegans* is correct, then it is reasonable to assume that *Elmisaurus rarus* possessed a similar mandible. In this case, the elongation of the hindlimbs in elmisaurines may be the result of ecological pressures for prey capture and herbivory.

Stratigraphic and geographic range.— *Elmisaurus rarus* has only been recovered from the Nemegt Formation of the Nemegt Locality of Mongolia.

Conclusions

The new specimens provide a great deal of new anatomical information. The frontal indicates the presence of a large nasal crest, and the tibia shows adaptations for extensive cursoriality. The distinctive tarsometatarsal anatomy indicates that *Elmisaurus rarus* and the North American *Leptorhynchos elegans* form a clade within Caenagnathidae. This clade, Elmisaurinae, is distinguished from Caenagnathinae by the fusion of the distal tarsals with each other and the proximal metatarsus, and by their smaller body size at maturity. Examination of hindlimb structure in Oviraptorosauria supports the existence of three distinct clades: a basal group with elongate feet but unfused tarsals; a derived group (caenagnathids) with elongate feet and fused tarsals (fused to the metatarsus in elmisaurines), and another derived group (oviraptorids) with short feet and unfused tarsals. Although only speculative, these differences may be linked to dietary and paleoecological differences between the groups.

Acknowledgements

Clive Coy (University of Alberta, Edmonton, Canada) carefully prepared the Mongolian specimens collected in 2000, and assisted with the photography. Eva Koppelhus (University of Alberta, Edmonton, Canada) photographed the specimens in Mongolia and helped in many other ways. The authors are grateful to Rinchen Barsbold and Khishigjaw Tsogtbaatar (Laboratory of Paleontology, Paleontological Center, Mongolian Academy of Sciences, Ulaan Baatar, Mongolia) and Tsogtbaatar Chinzorig (Laboratory of Paleontology, Paleontological Center, Mongolian Academy of Sciences,

Ulaan Baatar, Mongolia) for advice and access to specimens. Jackie Wilke and Brandon Striliski (both Royal Tyrrell Museum of Palaeontology, Drumheller, Canada) provided specimen data from the Tyrrell Museum. Four members of the "2000 Dinosaurs of the Gobi" expedition (Leigh Hunter, Charlie Lai, Jessica Lee, and Al Miniaci) provided funding that assisted with the collection and preparation of the new Mongolian specimens. The manuscript greatly benefited from the reviews by Amy Balanoff (Stony Brook University, New York, USA), Stephen Brusatte (University of Edinburgh, Scotland, United Kingdom), and Junchang Lu (Institute of Geology, Chinese Academy of Sciences).PJC and GFF are supported by NSERC, the second author is also funded by Alberta Innovates, and travel to Mongolia was funded in part by the Dinosaur Research Institute. This paper is dedicated to the memories of Halszka Osmólska and Demchig Badamgarav, two great women who made significant contributions to this study.

References

Anderson J.F., Hall-Martin A., and Russell D.A. 1985. Long-bone circumference and weight in mammals, birds and dinosaurs. Journal of Zoology, London A 207: 53–61.

Balanoff, A.M. and Norell, M.A. 2012. Osteology of Khaan mckennai (Oviraptoria: Theropoda). American Museum of Natural History, Bulletin 372: 1–77.

Barsbold, R. 1977. Kineticism and peculiarity of the jaw apparatus of oviraptors (Theropoda, Saurischia) [in Russian]. Joint Soviet-Mongolian Paleontological Expedition, Transactions 4: 37–47.

Barsbold, R. 1981. Toothless dinosaurs of Mongolia. Joint Soviet-Mongolian Paleontological Expedition, Transactions 15: 28–39.

Barsbold, R. 1983. Carnivorous dinosaurs from the Cretaceous of Mongolia [in Russian]. Joint Soviet-Mongolian Paleontological Expedition, Transactions 19: 1–120.

Barsbold, R. 1986. Rabdinosaurier Oviraptorenin. In: E.I. Vorobyeva (ed.),

Herpetologische Untersuchungen in der Mongolisch en Volskrepublik: 210–223. Akademia Nauk SSSR Institute Evolyucionnoy Morfologii i Ekologii Zhivotnich im. A.M. Severtsova, Moskva.

Benton, M.J. 2000. Conventions in Russian and Mongolian palaeontological literature. In: Benton, M.J., Shishkin, M.A., Unwin, D.M., and Kurochkin, E.N. (eds.), The Age of Dinosaurs in Russia and Mongolia, xvi–xxxix. Cambridge University Press, Cambridge.

Britt, B.B. 1993. Pneumatic Postcranial Bones in Dinosaurs and Other Archosaurs. 383 pp. Unpublished Ph.D. thesis, University Calgary, Calgary.

Brochu, C.A. 2002. Osteology of Tyrannosaurus rex: insights from a nearly complete skeleton and high-resolution computed tomographic analysis of the skull. Journal of Vertebrate Paleontology Memoir 7: 1–138.
http://dx.doi.org/10.2307/3889334

Chiappe, L.M., Ji S.-A., Ji Q., and Norell, M.A. 1999. Anatomy and systematics of the Confuciusornithidae (Theropoda: Aves) from the late Mesozoic of northeastern China. American Museum of Natural History, Bulletin 242: 1–89.

Clark, J.M., Norell, M.A., and Rowe T. 2002. Cranial anatomy of Citipati osmolskae (Theropoda, Oviraptorosauria), and a reinterpretation of the holotype of Oviraptor philoceratops. American Museum Novitates 3364: 1–24.
http://dx.doi.org/10.1206/0003-0082(2002)364<0001:CAOCOT>2.0.CO;2

Currie, P.J. 1989. The first records of Elmisaurus (Saurischia Theropoda) from North America. Canadian Journal of Earth Sciences 26: 1319–1324.
http://dx.doi.org/10.1139/e89-111

Currie, P.J. 1990. The Elmisauridae. In: D.B. Weishampel, P. Dodson, and H. Osmólska (eds.), The Dinosauria, 245–248. University of California Press, Berkeley.

Currie, P.J. 1997. Elmisauridae. In: P.J. Currie and K. Padian (eds.), Encyclopedia of Dinosaurs, 209–210. Academic Press, San Diego.

Currie, P. J. 2003. Allometric growth in tyrannosaurids (Dinosauria: Theropoda) from the Upper Cretaceous of North America and Asia. Canadian Journal of Earth Sciences 40: 651–665.
http://dx.doi.org/10.1139/e02-083

Currie, P.J., Godfrey, S.J., and Nessov, L. 1993. New caenagnathid (Dinosauria: Theropoda) specimens from the Upper Cretaceous of North America and Asia. Canadian Journal of Earth Sciences 30: 2255–2272. http://dx.doi.org/10.1139/e93-196

Currie, P.J. and Peng, J.H. 1993. A juvenile specimen of Saurornithoides mongoliensis from the Upper Cretaceous of northern China. Canadian Journal of Earth Sciences 30: 2224–2230. http://dx.doi.org/10.1139/e93-193

Currie, P.J. and Russell, D.A. 1988. Osteology and relationships of Chirostenotes pergracilis (Saurischia, Theropoda) from the Judith River (Oldman) Formation of Alberta, Canada. Canadian Journal of Earth Sciences 25: 972–986.

Funston, G.F. and Currie, P.J. 2014. A previously undescribed caenagnathid mandible from the late Campanian of Alberta, and insights into the diet of Chirostenotes pergracilis (Dinosauria: Oviraptorosauria). Canadian Journal of Earth Sciences 51: 156–165.
http://dx.doi.org/10.1139/cjes-2013-0186

Funston, G.F., Currie, P.J., and Burns, M.E. [in press]. New elmisaur specimens from Alberta, Canada, and their relationship to the Mongolian Elmisaurus rarus. Acta Palaeontologica Polonica.

Gilmore, C.W. 1924. Contributions to vertebrate palaeontology, notes on some unidentified vertebrae. Geological Survey (Department of Mines, Canada), Bulletin 38 (Geological Series 43): 9–12.

Gradziński, R., Kielan-Jaworowska, Z., and Maryańska, T. 1977 Upper Cretaceous Djadokhta, Barun Goyot and Nemegt formations of Mongolia, including remarks on previous subdivisions. Acta Geologica Polonica 27: 281–318.

Jasinoski, S.C., Russell, A.P., and Currie, P.J. 2006. An integrative phylogenetic and extrapolatory approach to the reconstruction of dromaeosaur (Theropoda: Eumaniraptora) shoulder musculature. Zoological Journal of the Linnean Society 146: 301–344.
http://dx.doi.org/10.1111/j.1096-3642.2006.00200.x

Ji, Q., Currie, P.J., Norell, M.A., and Ji, S.A. 1998. Two feathered dinosaurs from northeastern China. Nature 393: 753–761.
http://dx.doi.org/10.1038/31635

Kirkland, J.I., and Wolfe, D.G. 2001. First definitive therizinosaurid (Dinosauria: Theropoda) fromNorth America. Journal of Vertebrate Paleontology 21: 410–414.
http://dx.doi.org/10.1671/0272-4634(2001)021[0410:FDTDTF]2.0.CO;2

Kurzanov, S.M. 1981. An unusual theropod from the Upper Cretaceous of Mongolia [in Russian]. Joint Soviet-Mongolian Paleontological Expedition 15: 39–49.

Lamanna, M.C., Sues, H.D., Schachner, E.R., and Lyson, T.R. 2014. A new large-bodied oviraptorosaurian theropod dinosaur from the latest Cretaceous of western North America. PLoS One 9 (3): e92022. http://dx.doi.org/10.1371/journal.pone.0092022

Longrich, N.R., Barnes, K., Clark, S., and Millar, L. 2013. Caenagnathidae from the Upper Campanian Aguja Formation of West Texas, and a revision of the Caenagnathinae. Peabody Museum of Natural History, Bulletin 54: 23–49.

Lu, J.-C., Currie, P.J., Xu, L., Zhang, X.-L., Pu, H.-Y., and Jia, S.-H. 2013. Chicken-sized oviraptorid dinosaurs from central China and their ontogenetic implications. Naturissenschaften 100: 165–175. http://dx.doi.org/10.1007/s00114-012-1007-0

Montanari, S., Higgins, P., and Norell, M.A. 2013. Dinosaur eggshell and tooth enamel geochemistry as an indicator of Mongolian Late Cretaceous paleoenvironments. Palaeogeography, Palaeoclimatology, Palaeoecology 370: 158–166. http://dx.doi.org/10.1016/j.palaeo.2012.12.004

Norell, M.A. and Makovicky, P.J. 1997. Important features of the dromaeosaur skeleton: information from a new specimen. American Museum of Natural History, Novitates 3215: 1–28.

Osmólska, H. 1981. Coossified tarsometatarsi in theropod dinosaurs and their bearing on the problem of bird origins. Palaeontologia Polonica 42: 79–95.

Osmólska, H. 1996. An unusual theropod dinosaur from the Late Cretaceous Nemegt Formation of Mongolia. Acta Palaeontologica Polonica 41 (1): 1–38.

Osmólska, H. 2004. Evidence on relation of brain to endocranial cavity in oviraptorid dinosaurs. Acta Palaeontologica Polonica 49 (2): 321–324.

Osmólska, H., Roniewicz, E., and Barsbold, R. 1972. A new dinosaur, Gallimimus bullatus n. gen., n. sp. (Ornithomimidae) from the Upper Cretaceous of Mongolia. Palaeontologia Polonica 27: 103–143.

Ostrom, J.H. 1976. On a new specimen of the Lower Cretaceous theropod dinosaur Deinonychus antirrhopus. Breviora 439: 1–21.

Perle, A. 1979. Segnosauridae—a new family of theropods from the Late Cretaceous of Mongolia. Joint Soviet-Mongolian Paleontological Expedition, Transactions 8: 45–55.

Smith, D. 1992. The type specimen of Oviraptor philoceratops, a theropod dinosaur from the Upper Cretaceous of Mongolia. Neues Jahrbuch für Geologie und Paläontologie Abhandlungen 186: 365–388.

Sternberg, C.M. 1932. Three new theropod dinosaurs from the Belly River Formation of Alberta. Canadian Field Naturalist 46: 99–105.

Sues, H.-D. 1997. On Chirostenotes, a Late Cretaceous oviraptorosaur (Dinosauria: Theropoda) from western North America. Journal of Vertebrate Paleontology 17: 698–716.
http://dx.doi.org/10.1080/02724634.1997.10011018

Sullivan, R.M., Jasinski, S.E., and Van Tomme, M.P.A. 2011. A new caenagnathid Ojoraptorsaurus boerei, n.gen., n. sp. (Dinosauria, Oviraptorosauria), from the Upper Cretaceous Ojo Alamo Formation (Naashoibito Member, San Juan Basin, New Mexico. New Mexico Museum of Natural History and Science, Bulletin 53: 418–428.

Zanno, L.E., and Sampson, S.D. 2005. A new oviraptorosaur (Theropoda, Maniraptora) from the Late Cretaceous (Campanian) of Utah. Journal of Vertebrate Paleontology 25 (4): 897–904.
http://dx.doi.org/10.1671/0272-4634(2005)025[0897:ANOTMF]2.0.CO;2

Table 1. Measurements (in mm) of *Elmisaurus rarus*. Square brackets, measurements previously published by Osmólska (1981); [e], estimated.

	MPC-D 102/006	MPC-D 102/007	ZPAL MgD-I/ 98
Frontal: length	–	50.5	–
interorbital distance	–	26.2	–
intertemporal distance	–	25.0	–
maximum width	–	21.5	–
cervical centrum: length	–	25.5	–
minimum height, midlength	–	15.5	–
neural canal diameter	–	8.0	–
pleuocoel dimensions	–	2.5 x 5.0	–
anterior dorsal vertebra: centrum L	–	28.9	–
width of centrum, posterior	–	20.0	–
diameter of neural canal	–	7.8	–
pleurocoel dimensions	–	7.8 x 3.4	–
mid-sacral centrum: length	–	–	37.0
width	–	–	19.0
Metacarpal I, length	–	–	[45.0]
Metacarpal II, length	–	–	?
Metacarpal III, length	–	–	–
Manual phalanx I-1 length	–	–	[65.0]
Manual phalanx I-2 (ungual), length	–	–	[44.0]
Manual phalanx II-1	–	–	[66.0]
Manual phalanx II-2	–	44+	[66.0]
Manual phalanx II-3 (ungual)	–	40	–
Manual phalanx III-1	–	28	[30.0]
Manual phalanx III-2	–	–	[30.0]
Manual phalanx III-3	–	40	[43.0]
Manual phalanx III-4 (ungual)	–	–	–
Femur, length	–	246.0[e]	308.0[e]
Femur, anteroposterior shaft width	–	26.6	28.0
Femur, transverse shaft width	–	25.2	27.7
Femur, shaft circumference	–	70.0	99
Tibia, length	–	323.0	340.0[e]
Tibia, lateromedial shaft width	–	25.3	30.0
Tibia, anteroposterior shaft width	–	19.0	24.0
Tarsometatarsus, maximum length	194.0	276e	–
Tarsometatarsus, proximal width	49.3	45.8	–
Metatarsal I, length	–	–	–
Metatarsal II, length	172.4	161.8	–
Metatarsal III, length	185.0	172e	–
Metatarsal IV, length	175.7	162.2	–
Metatarsal V, length	69.0	–	–
Pedal phalanx I-1	–	23.1	26.0
Pedal phalanx I-2 (ungual)	–	30	23.0[e]
Pedal phalanx II-1	–	–	45.0
Pedal phalanx II-2	–	–	34.0
Pedal phalanx II-3 (ungual)	–	–	31.0[e]
Pedal phalanx III-1	–	–	46.0
Pedal phalanx III-2	–	–	32.0
Pedal phalanx III-3	–	–	30.0
Pedal phalanx III-4 (ungual)	–	–	?

		MPC-D	ZPAL MgD-I/
Pedal phalanx IV-1	–	–	28.0+
Pedal phalanx IV-2	–	–	22.0
Pedal phalanx IV-3	–	–	19.0
Pedal phalanx IV-4	–	–	18.0
Pedal phalanx IV-5 (ungual)	–	–	26.0[e]

Table 2. Manus measurements (in mm) of some maniraptorans. A, *Chirostenotes pergracilis* CMN 2367; B, *Chirostenotes pergracilis* TMP 1979.020.0001; C, *Elmisaurus rarus* ZPAL MgD-I/98; D, *Sinornithoides youngi* IVPP V9612; E, *Citipati* n. sp. MPC-D 100/42; F, *Oviraptor philoceratops* AMNH 6517; G, *Conchoraptor gracilis* MPC-D 100/38, /39; H, *Ingenia yanshini* MPC-D 100/30, /31; I, *Deinonychus antirrhopus* YMP 5206; J, *Velociraptor mongoliensis* MPC-D 100/982, /25, /unnumbered. Abbreviations: [e], estimate; Mc, metacarpal.

	A	B	C	D	E	F	G	H	I	J
Mc I	?	?	45	11.7	47	?	23/23[e]	30/31	45.8	19.2/25/26
I-1	63	73	65	29.0	95	79	37+/41	42/37	74.1	39.9[e]/44/49
I-2	49	47[e]	?	22.5	73	62+	26[e]/27[e]	50/47	?	39.9[e]/47/46
Mc II	?	?	?	33.5	100+	95	42/?	46/46	88.3[e]	50.8/58/56
II-1	65	81	66	18.5	58	54	20+/?	25/21	54.0	31.3/35/37
II-2	72	87	66	28.5	73	68	28/31[e]	20/20	76.5	45.8/48/52
II-3	63	73	51[3]	22.0	64	47e	20[e]/23[e]	28/24[e]	?	?/51[e] /37[e]
McIII	?	?	?	33.0	98	90	43[e]/44	43[e]/44	82.0	45/50/50
III-1	?	36	30	4.2	42	39	17/?	17/15	29.9	17.6/20/20
III-2	?	?	30	8.6	40	37	21/?	11/8	20.5	10.1/12/14
III-3	44	45	43	20.3	56	58	24[e]/24[e]	10/3	58[e]	32.2/35/36
III-4	39	?	?	17.3	54	50+	22[e]/20	17/?	?/?	32.0/33/30

Table 3. Phalangeal proportions in maniraptoran manus.

II-1/II-2 length ratio:		
Chirostenotes pergracilis	0.90-0.93	
Elmisaurus rarus	1.00	
Sinornithoides youngi		0.65
Citipati n.sp.		0.79
Oviraptor philocertops	0.79	
Conchoraptor gracilis		0.80
Ingenia yanshini	1.08	
Deinonychus antirrhopus	0.70	
Velociraptor mongoliensis		0.68-0.73
III-1/III-3 length ratio:		
Chirostenotes pergracilis	0.80	
Elmisaurus rarus	0.70	
Sinornithoides youngi		0.84
Citipati n.sp.		0.75
Oviraptor philoceratops	0.67	
Conchoraptor gracili		0.71
Ingenia yanshini	05.0	
Deinonychus antirrhopus	0.60	
Velociraptor mongoliensis	0.55-0.57	
II-3/(II-1+II-2+II-3) length ratio:		
Chirostenotes pergracilis	0.30	
Elmisaurus rarus	0.28	
Sinornithoides youngi		0.32
Citipati n.sp.		0.33
Oviraptor philoceratops	0.28	
Conchoraptor gracilis		0.28
Ingenia yanshini	0.38	
Deinonychus antirrhopus	0.34	
Velociraptor mongoliensis	0.34-0.35	
II-1/II-2 length ratio:		
Elmisaurinae		0.90-1.0
Troodontidae		0.65
Oviraptorinae		0.79-0.80
Ingeniinae		1.05-1.25
Dromaeosauridae	0.68-0.73	
III-1/III-3 length ratio:		
Elmisaurinae		0.70-0.80
Troodontidae		0.84
Oviraptorinae		0.67-0.75
Ingeniinae		1.70-5.00
Dromaeosauridae	0.55-0.60	
II-3/(II-1+II-2+II-3) length ratio:		
Elmisaurinae		0.28-0.30
Troodontidae:		0.32
Oviraptorinae		0.28-0.33
Ingeniinae		0.37-0.38
Dromaeosauridae	0.34	

Figures

Fig. 1. Crested theropod dinosaur *Elmisaurus rarus* Osmólska, 1981, MPC-D 102/007 from Western Sayr of Nemegt Locality, Nemegt Formation (Upper Cretaceous). Right frontal in dorsal (**A**), medial (**B**), anterior (**C**), posterior (**D**), ventral (**E**), and lateral (**F**) views. Abbreviations: end, endocranial cavity; intf, interfrontal suture; nas, nasal suture; orb, orbit; par, parietal suture; pop, postorbital process.

Fig. 2. Crested theropod dinosaur *Elmisaurus rarus* Osmólska, 1981, MPC-D 102/007 from Western Sayr of Nemegt Locality, Nemegt Formation (Upper Cretaceous). Anterior dorsal vertebra in right lateral (**A**), left lateral (**B**), dorsal (**C**), anterior (**D**), and posterior (**E**) views. Abbreviations: hyp, hyposphene/hypantrum; pa, parapophysis; 1, infrapostzygapophysial pneumatic fossa; 2, infradiapophysial pneumatic fossa; 3, infraprezygapophysial pneumatic fossa; 4, pleurocoel.

Fig. 3. Crested theropod dinosaur *Elmisaurus rarus* Osmólska, 1981, MPC-D 102/007 from Western Sayr of Nemegt Locality, Nemegt Formation (Upper Cretaceous). **A**. ?first dorsal rib. **B**. Anterior dorsal rib. **C**. Posterior dorsal rib. 1, pneumatopore.

Fig. 4. Crested theropod dinosaur *Elmisaurus rarus* Osmólska, 1981, Z-PAL MgD-I/98 from Northern Sayr of Nemegt Locality, Nemegt Formation (Upper Cretaceous). Proximal portion of right scapula in lateral view (**A**); proximal portion of right ischium in lateral view (**B**); proximal head of left femur in anterior view (**C**); distal end of right tibia in posterior view (**D**). Not to scale. Abbreviations: acr, acromion process; gl, glenoid; h, femoral head; ob, obturator process; pff, postfibular flange; tc, trochanteric crest.

Fig. 5. Crested theropod dinosaur *Elmisaurus rarus* Osmólska, 1981, MPC-D 102/007 from Western Sayr of Nemegt Locality, Nemegt Formation (Upper Cretaceous). Manual phalanges II-2 (**A**, **F**, **N**), II-3 (**B**, **E**, **M**), III-1 (**D**, **G**, **H**, **K**) and III-3 (**C**, **I**, **J**, **L**). F, G, I in proximal view, E, H, J in distal aspect. E to J not to scale.

Fig. 6. Crested theropod dinosaur *Elmisaurus rarus* Osmólska, 1981, MPC-D 102/007 from Western Sayr of Nemegt Locality, Nemegt Formation (Upper Cretaceous). Proximal head of femur in anterior (**A**) and medial (**B**) views. Tibia in anterior (**C**, **G**), proximal (**E**), distal (**F**) and lateral views (**D**, **H**). Abbreviations: cn, cnemial crest; fib, fibular condyle; h, head of femur; int, crest for interosseum tibiofibular ligament; pff, postfibular flange; tc, trochanteric crest.

Fig. 7. Crested theropod dinosaur *Elmisaurus rarus* Osmólska, 1981, MPC-D 102/006 from Western Sayr of Nemegt Locality, Nemegt Formation (Upper Cretaceous). Right tarsometatarsus (**A**, **G**); MPC-D 102/007, left tarsometatarsus (**B**–**F**). Tarsals in dorsal

(**A**, **B**), anterior (**C**), lateral (**D**), posterior (**E**), and medial (**F**) views. Contact between distal tarsal IV and fifth metatarsal (G). Abbreviations: dt III, third distal tarsal; dt IV, fourth distal tarsal; MT II, second metatarsal; MT V, fifth metatarsal.

Fig. 8. Crested theropod dinosaur *Elmisaurus rarus* Osmólska, 1981, MPC-D 102/006 (**A**, **B**, **G**), MPC-D 102/007 (**C**, **D**, **E**, **H**), MPC-D 102/008 (**F**) from Western Sayr of Nemegt Locality, Nemegt Formation (Upper Cretaceous). Tarsometatarsals in anterior (**A**, **C**, **F**), posterior (**B**, **D**), lateral (**E**), and distal (**G**, **H**) views. In C and D, the left metatarsal III has been mirrored and associated with the right metatarsi II and IV. Abbreviations: atp, slit for a. tarsalis plantaris; cr, cruciate ridges; dt III, third distal tarsal; mtc, insertion of m. tibialis cranialis; mt III, facet for third metatarsal; mt IV, facet for fourth metatarsal; MT V, fifth metatarsal; pdp, posterodorsal process of fourth distal tarsal; plr, posterolateral ridge of fourth metatarsal; pmr, posteromedial ridge of second metatarsal; vs, vascular slit.

Fig. 9. Crested theropod dinosaur *Elmisaurus rarus* Osmólska, 1981 from Western Sayr of Nemegt Locality, Nemegt Formation (Upper Cretaceous). Cross section of MPC-D 102/006 (a third of the tarsometatsus length from the proximal end), showing the deep plantar trough. Abbreviations: II, second metatarsal; III, third metatarsal; IV, fourth metatarsal.

Fig. 10. Crested theropod dinosaur *Elmisaurus rarus* Osmólska, 1981 from Western Sayr of Nemegt Locality, Nemegt Formation (Upper Cretaceous). MPC-D 102/006 and MPC-D 102/007, demonstrating the cruciate ridges on the posterior surface of the third metatarsal. Abbreviations: cr, cruciate ridges.

Fig. 11. Crested theropod dinosaur *Elmisaurus rarus* Osmólska, 1981, MPC-D 102/007 from Western Sayr of Nemegt Locality, Nemegt Formation (Upper Cretaceous). Pedal phalanges I-1 (**A**–**E**) and I-2 (**F**, **G**) in proximal (**A**, **F**), dorsal (**B**), lateral (**C**, **G**), distal (**D**), and ventral (**E**) views.

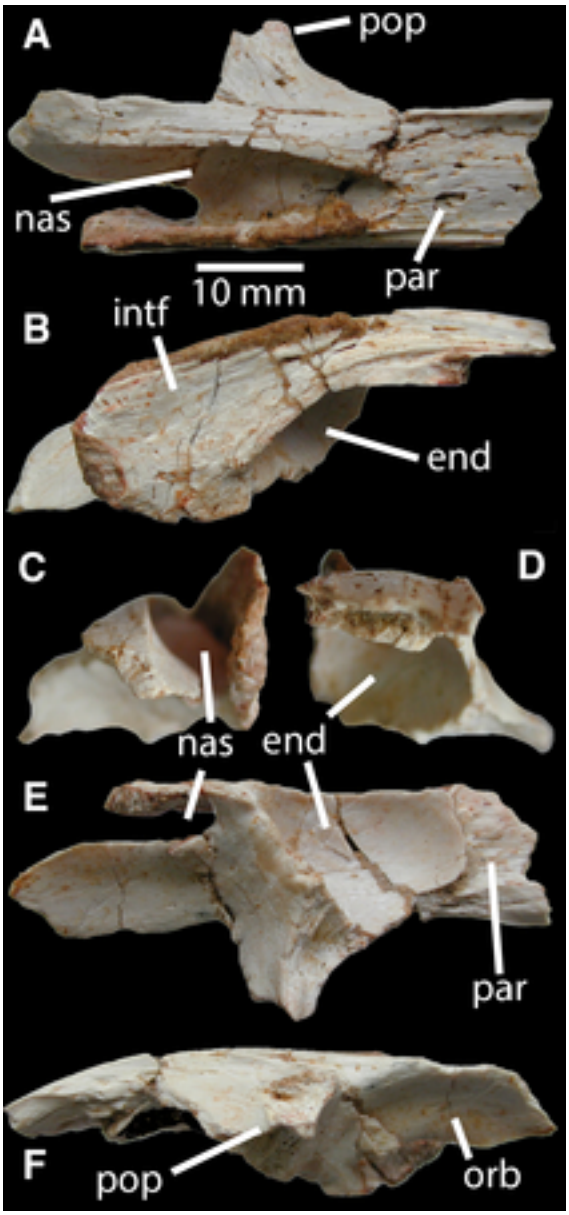

Fig. 1. Elmisaurus rarus, MPC-D 102/007. Right frontal in dorsal (A), medial (B), anterior (C), posterior (D), ventral (E) and lateral (F) views. Abbreviations: end, endocranial cavity; intf, interfrontal suture; nas, nasal suture; orb, orbit; par, parietal suture; pop, postorbital process.

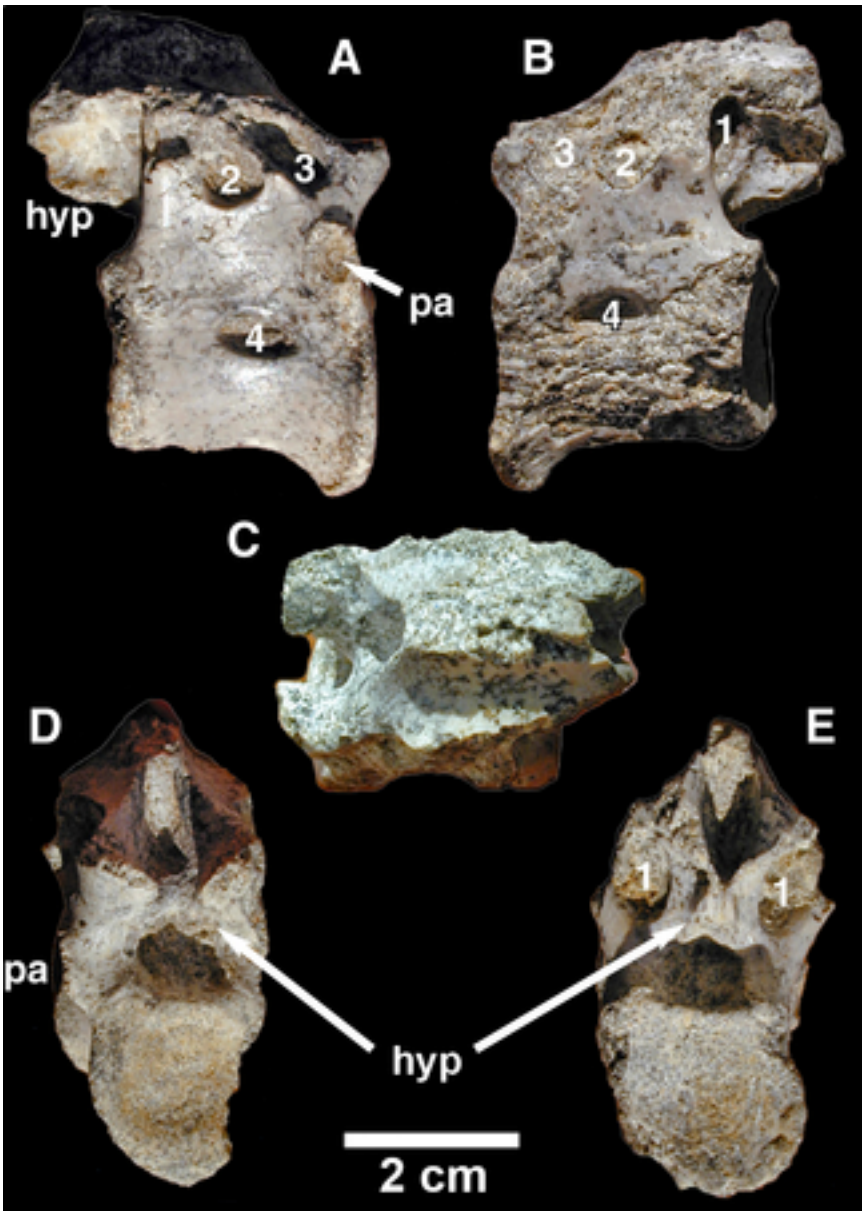

Fig. 2. Elmisaurus rarus, MPC-D 102/007. Anterior dorsal vertebra in right lateral (A), left lateral (B), dorsal (C), anterior (D) and posterior (E) views. Abbreviations: hyp, hyposphene/hypantrum; pa, parapophysis; 1, infrapostzygapophysial pneumatic fossa; 2, infradiapophysial pneumatic fossa; 3, infraprezygapophysial pneumatic fossa; 4, pleurocoel.

Fig. 3. Elmisaurus rarus, MPC-D 102/007. A, ?first dorsal rib; B, anterior dorsal rib; C, posterior dorsal rib. 1, pneumatopore.

Fig. 4. Elmisaurus rarus, Z-PAL MgD-I/98, Proximal portion of right scapula in lateral view (A); proximal portion of right ischium in lateral view (B); proximal head of left femur in anterior view (C); distal end of right tibia in posterior view (D). Not to scale. Abbreviations: acr, acromion process; gl, glenoid; h, femoral head; ob, obturator process; pff, postfibular flange; tc, trochanteric crest.

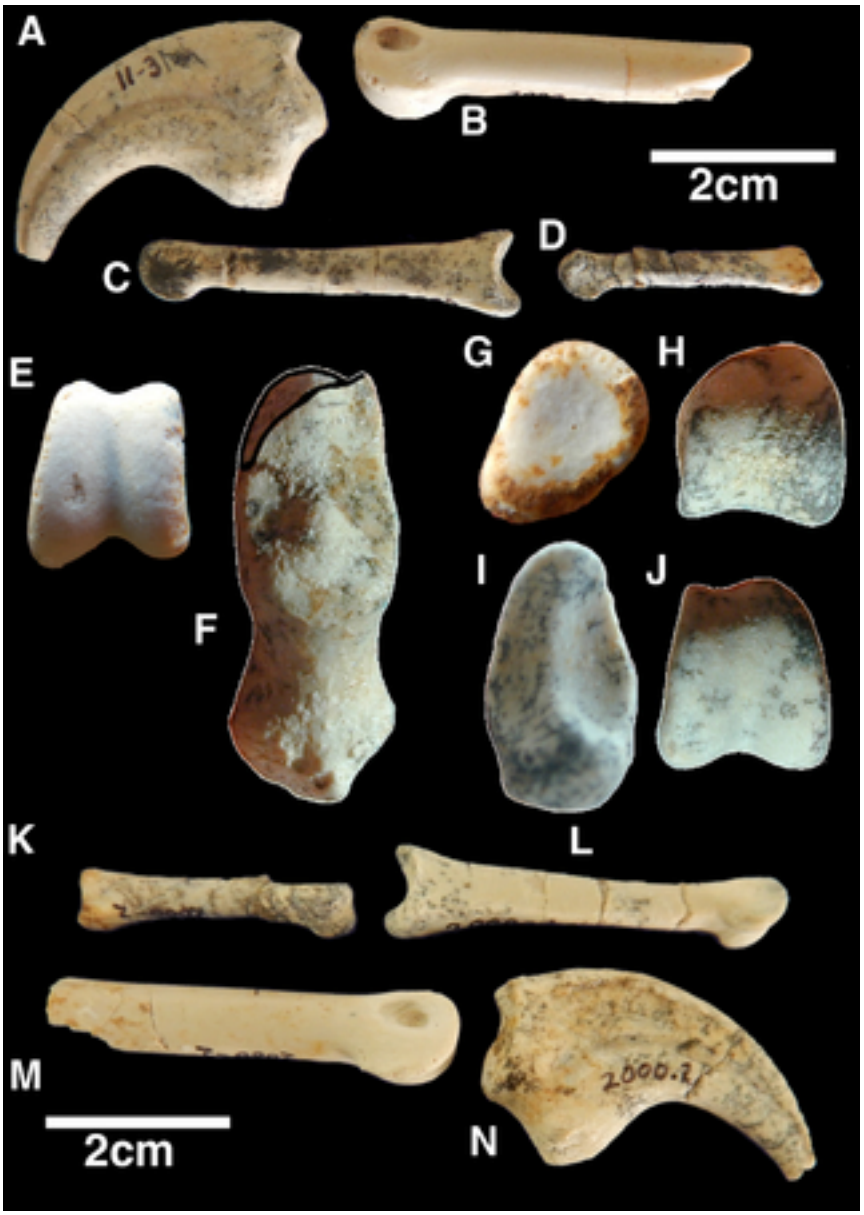

Fig. 5. Elmisaurus rarus, MPC-D 102/007. Manual phalanges II-2 (A, F, N), II-3 (B, E, M), III-1 (D, G, H, K) and III-3 (C, I, J, L). F, G, I in proximal view, E, H, J in distal aspect. E to J not to scale.

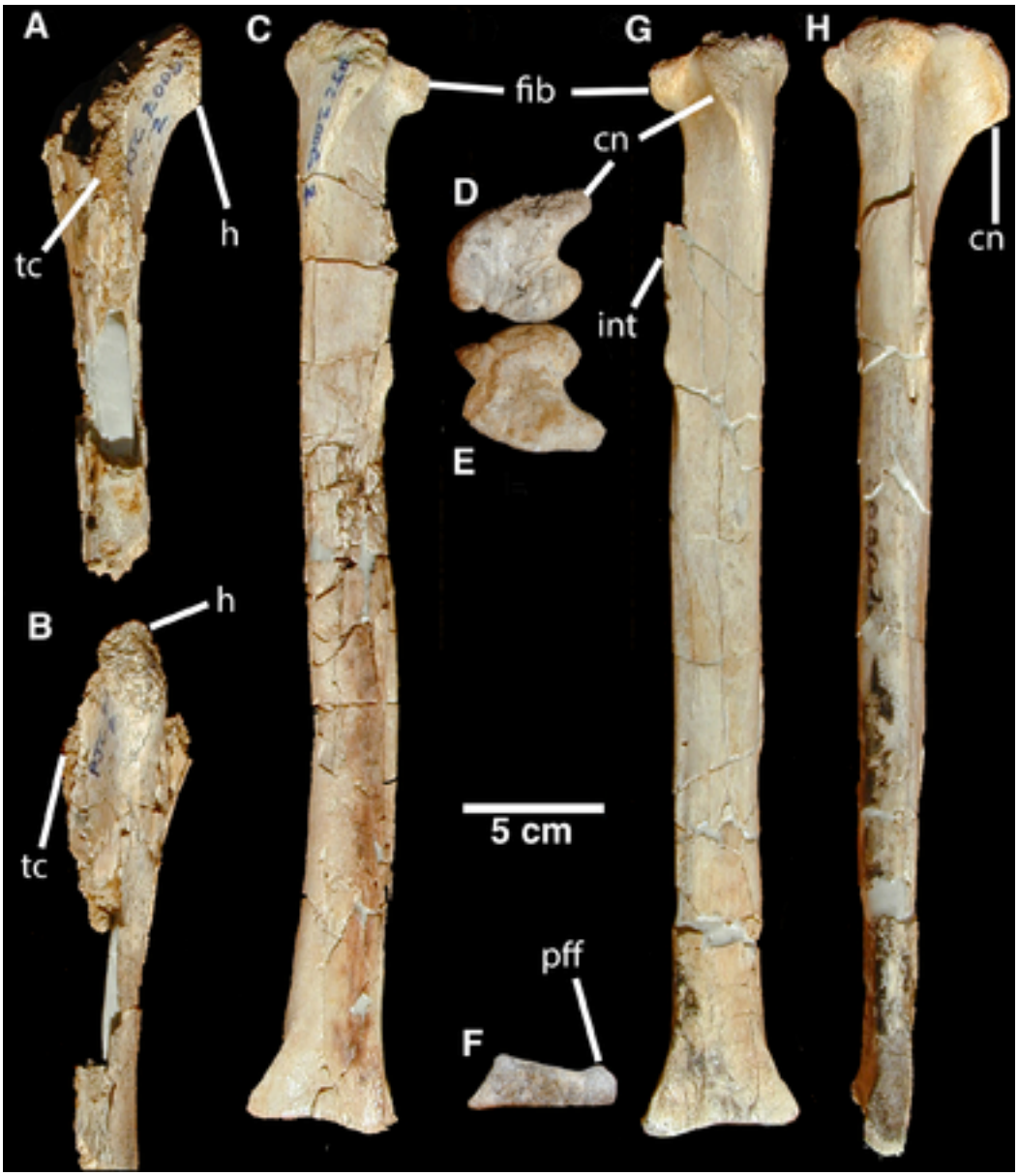

Fig. 6. Elmisaurus rarus, MPC-D 102/007. Proximal head of femur in anterior (A) and medial (B) views. Tibia in anterior (C, G), proximal (E), distal (F) and lateral views (D, H). Abbreviations: cn, cnemial crest; fib, fibular condyle; h, head of femur; int, crest for interosseum tibiofibular ligament; pff, postfibular flange; tc, trochanteric crest.

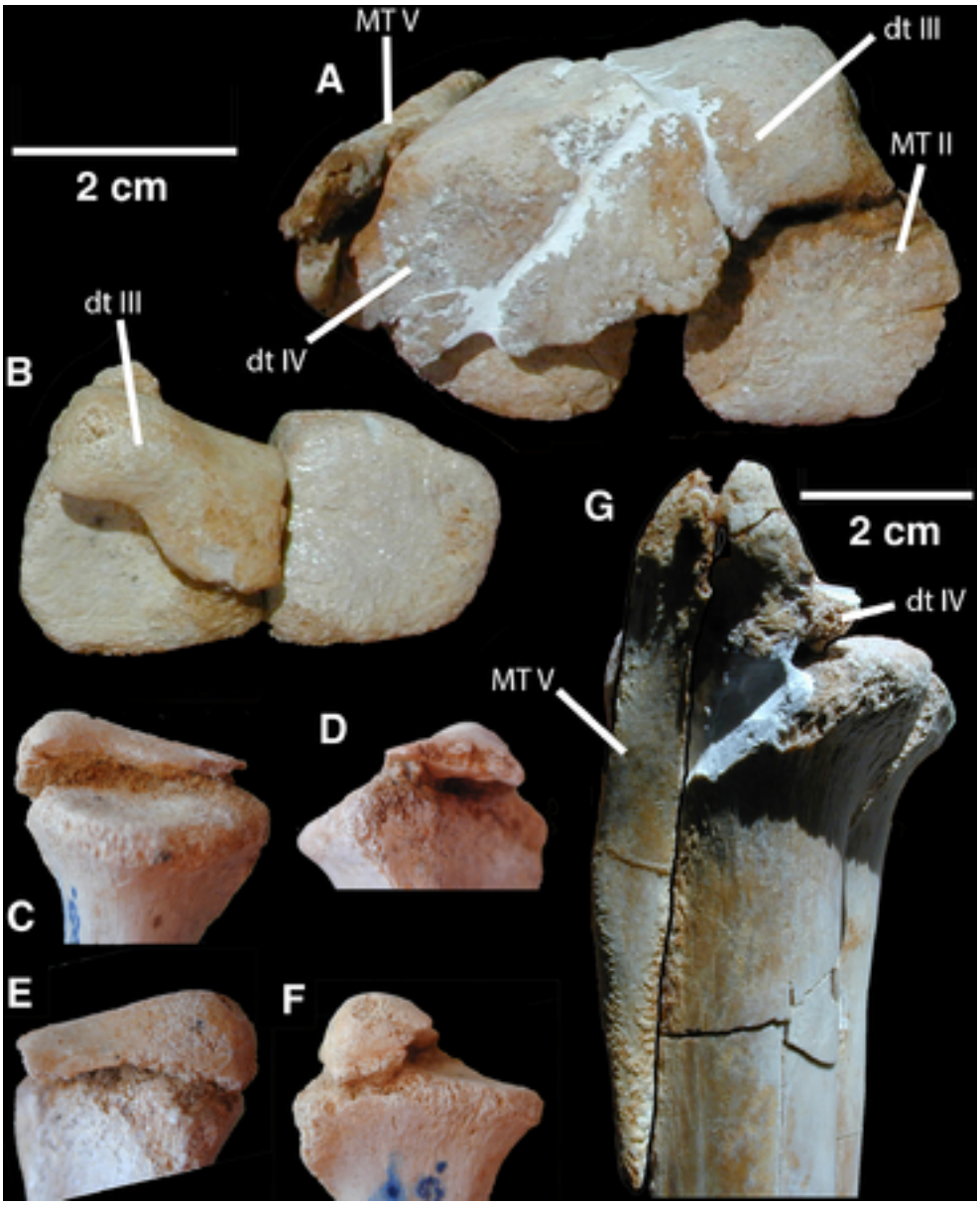

Fig. 7. Elmisaurus rarus. MPC-D 102/006, right tarsometatarsus (A, G); MPC-D 102/007, left tarsometatarsus (B, C, D, E, F). Tarsals in dorsal (A, B), anterior (C), lateral (D), posterior (E), and medial (F) views. Contact between distal tarsal IV and fifth metatarsal (G). Abbreviations: dt III, third distal tarsal; dt IV, fourth distal tarsal; MT II, second metatarsal; MT V, fifth metatarsal.

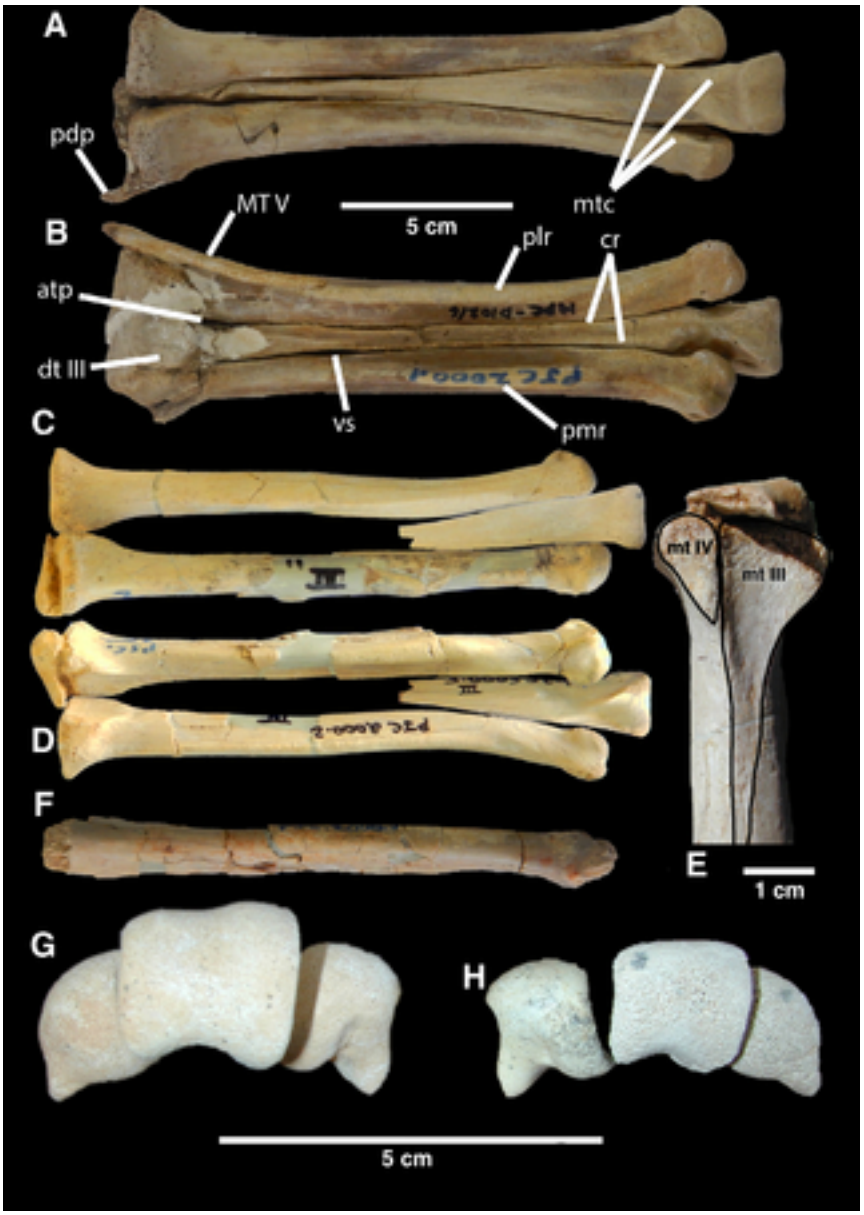

Fig. 8. Elmisaurus rarus, MPC-D 102/006 (A, B, G), MPC-D 102/007 (C, D, E, H), MPC-D 102/008 (F). Tarsometatarsals in anterior (A, C, F), posterior (B, D), lateral (E), and distal (G, H) views. In C and D, the left metatarsal III has been mirrored and associated with the right metatarsi II and IV. Abbreviations: atp, slit for a. tarsalis plantaris; cr, cruciate ridges; dt III, third distal tarsal; mtc, insertion of m. tibialis cranialis; mt III, facet for third metatarsal; mt IV, facet for fourth metatarsal; MT V, fifth metatarsal; pdp, posterodorsal process of fourth distal tarsal; plr, posterolateral ridge of fourth metatarsal; pmr, posteromedial ridge of second metatarsal; vs, vascular slit.

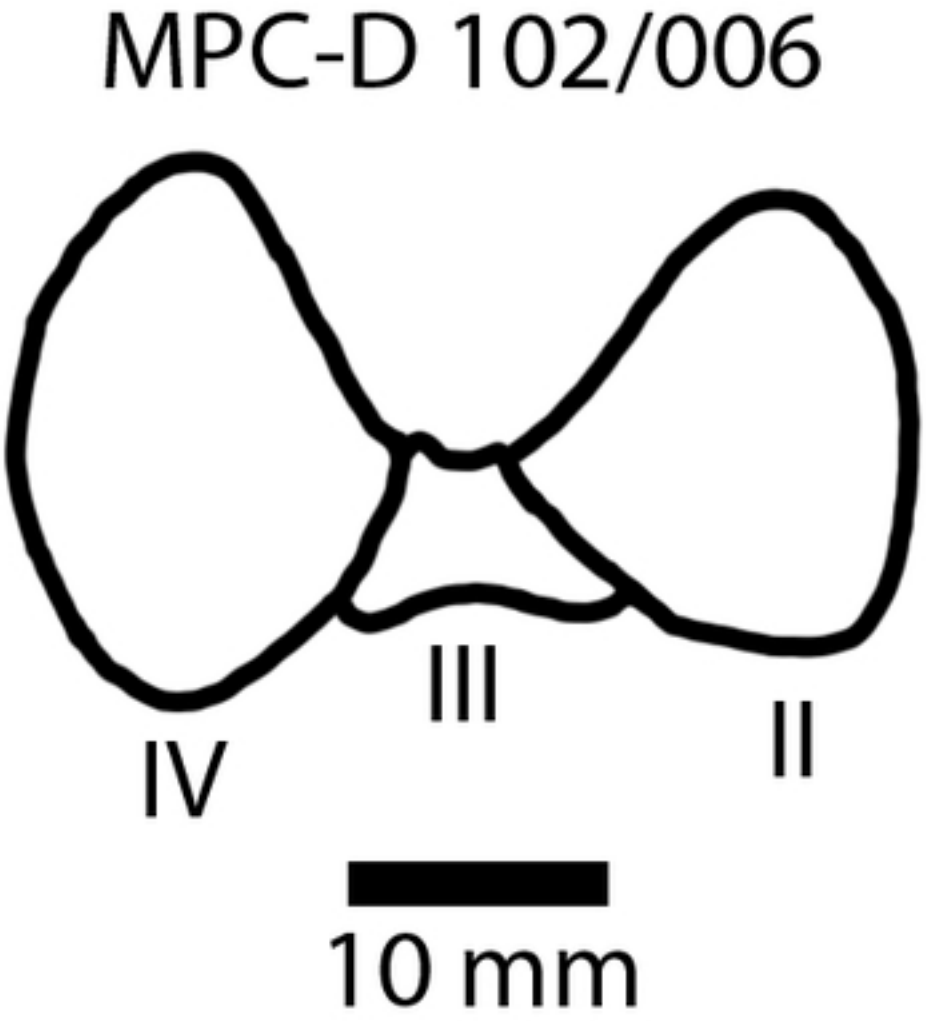

Fig. 9. Elmisaurus rarus, cross section of MPC-D 102/006 (a third of the tarsometatsus length from the proximal end), showing the deep plantar trough. Abbreviations: II, second metatarsal; III, third metatarsal; IV, fourth metatarsal.

Fig. 10. Elmisaurus rarus, MPC-D 102/006 and MPC-D 102/007, demonstrating the cruciate ridges on the posterior surface of the third metatarsal. Abbreviations: cr, cruciate ridges.

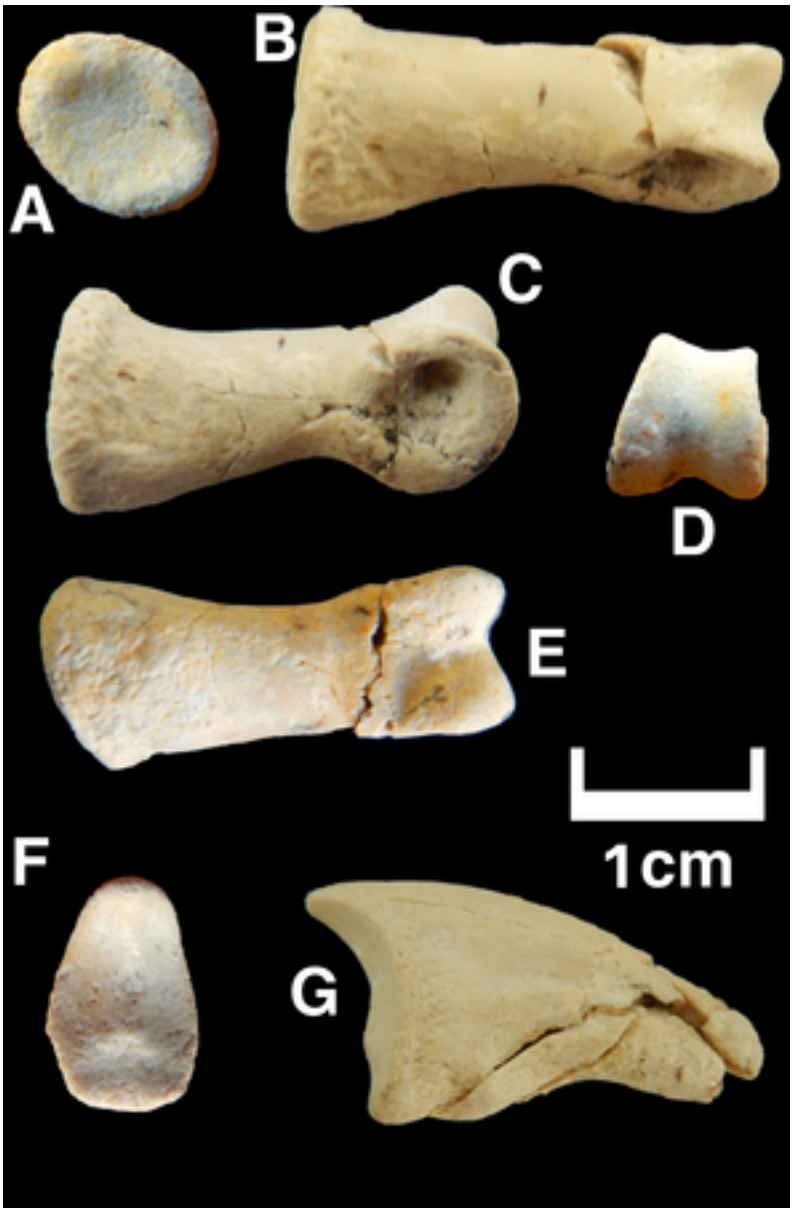

Fig. 11. Elmisaurus rarus, MPC-D 102/007. Pedal phalanges I-1 (A, B, C, D, E) and I-2 (F, G) in proximal (A, F), dorsal (B), lateral (C, G), distal (D) and ventral (E) views.